Pergamon

Int. J. Heat Mass Transfer. Vol. 41, No. 17, pp. 2667–2675, 1998

Printed in Great Britain
0017–9310/98 \$19.00+0.00

PII: S0017–9310(97)00262–7

Oscillatory instability analysis of Bénard–Marangoni convection in a rotating fluid under a uniform magnetic field

FU-PING CHANG and KO-TA CHIANG

Department of Mechanical Engineering, Shu-Teh Junior College of Technology and Commerce, Taichung, Taiwan 402, R.O.C.

(*Received* 29 *April* 1997 *and in final form* 28 *August* 1997)

Abstract—The effects of rotation and magnetic field on the onset of oscillatory modes of Bénard–Marangoni instability in a horizontal fluid layer with a deformably free surface are investigated numerically. The derived eigenvalue equations are solved using the fourth order Runge–Kutta–Gill's method coupled with the Broyden's method. The results show that the Crispation number C, associated with the deformation of the upper surface, is significant on the Bénard–Marangoni instability. The system is stabilizing, as the Biot number Bi, the Bond number Bo, the Taylor number $\mathscr{T}$ and the Chandrasekhar number Q increase. The absolute value of critical Marangoni number $|M_c|$ in the $(|M_c|, R)$-plane decreases linearly with increasing Rayleigh number R.

INTRODUCTION

A horizontal fluid layer with its upper surface deformably free is heated from below, the convective instability might set in as a result of the thermal buoyancy, the thermal variation of the surface tension or both, correspondently the Rayleigh–Bénard instability [1–4] the Marangoni instability [5, 6] or the Bénard–Marangoni instability [7–10]. The Bénard–Marangoni instability has received much consideration in many engineering problems, the oil extraction from a porous media, the energy storage in molten salts, the crystal growth in space and paints, colloids and detergents in chemical engineering. In reality, a free surface is subject to deformation under normal and shear stresses, unless the surface tension is infinitely strong. Scriven and Sternling [8] and Smith [9] studied the cases with the upper surface free and nondeformable. While Davis and Homsy [10] considered the deformable one.

The analyses above were limited to cases of stationary modes with oscillatory ones ignored. Taking into account the Crispation effect, the appearance of oscillatory modes became possible [11, 12]. For either Rayleigh–Bénard instability or Marangoni instability, the effect of rotation is a stabilizing factor [1, 13–15]. An extra effect of a uniform magnetic field is added to the problem [16–22]. The primary objective of the study does include effects of both rotation and magnetic field to the onset of oscillatory modes of the Bénard–Marangoni instability. In the linear stability theory we take the small disturbances in the form of $\exp(\sigma t)$, where t is the time. And $\sigma = \sigma_r + i\sigma_i$ is the reaction of the disturbances to the system, σ_r is the growth rate and σ_i is the frequency, respectively. If $\sigma_i \neq 0$ when $\sigma_r = 0$, there is the state of oscillatory instability mode and the disturbances will oscillate in time with no increase in infinitesimal amplitude [2, 3, 11, 12, 17, 20–22]. In this study, we calculate the critical Marangoni number M_c and frequency σ_i as function of the effects of rotation and magnetic field on the onset of an oscillatory modes of Bénard–Marangoni instability. The effects of Crispation number C at a deformable upper free surface and relevant physical parameter of fluid layer are also considered.

MATHEMATICAL FORMULATION

An infinitely horizontal fluid layer of thickness L, subject to a uniform rotation about the vertical axis with the angular velocity Ω and a uniform vertical magnetic field $\mathbf{H} = (0, 0, H)$, is considered, as shown in Fig. 1. The lower boundary of the fluid layer is bounded with an isothermal and rigid slab of temperature T_s. The upper boundary is deformably free and the variation of surface tension γ with the temperature T is assumed [6–12, 16, 18–22],

$$\gamma = \gamma_0 - \tau(T - T_0) \tag{1}$$

where γ_0 and T_0 are referential values of surface tension and temperature, respectively, and τ is the rate of change with the temperature. The equation of state for the density ρ is

$$\rho = \rho_0[1 - \alpha(T - T_0)] \tag{2}$$

where α is the coefficient of thermal expansion and ρ_0 is the density at the reference temperature T_0. The kinematic viscosity ν, thermal diffusivity κ, conductivity K, magnetic permeability μ and electrical resistivity η are assumed independent of the tempera-

NOMENCLATURE

a	wavenumber of the small disturbance
Bi	Biot number, hL/K
Bo	Bond number, $\rho g L^2/\gamma$
C	Crispation number, $\rho\nu\kappa/\gamma L$
g	gravitational acceleration
h	heat transfer coefficient
$\mathbf{H}$	magnetic field
H	z-component of magnetic field
K	thermal conductivity
L	thickness of fluid layer
M	Marangoni number, $\tau\Delta TL/\rho\nu\kappa$
Pr	Prandtl number, ν/κ
Q	Chandrasekhar number, $\mu H^2L^2/\rho\nu\eta$
R	Rayleigh number, $\alpha g\Delta TL^3/\nu\kappa$
t	time
T	temperature
T_s	temperature at bottom wall
$\mathscr{T}$	Taylor number, $4\Omega^2L^4/\nu^2$
w	z-dependent amplitude of velocity
W	z-dependent normal mode amplitude of non-dimensional velocity
x, y, z	coordinates
Z	magnitude of the disturbance of the nondimensional surface deflection.

Greek symbols

α	thermal expansion coefficient of the fluid density
γ	surface tension
ΔT	the difference of temperature across the fluid layer
ζ	z-dependent normal mode amplitude of nondimensional vertical velocity
η	electrical resistivity
θ	magnitude of the disturbance of temperature
Θ	normal mode magnitude of the disturbance of nondimensional temperature
κ	thermal diffusivity
μ	magnetic permeability
ν	kinematic viscosity of fluid
$\xi(x, y, t)$	position of the upper free surface
ρ	density of fluid
τ	surface tension gradient with respect to temperature, $\partial\gamma/\partial T$
σ_r, σ_i	real and imaginary growth rates with time
Ω	uniform angular velocity.

Subscript

o	referential quantity
c	critical state.

Superscript

$'$	perturbed quantity.

ture, except for surface tension γ and density ρ. The Boussinesq approximation is assumed (except for the surface tension) to be varying with the temperature [1–5, 7, 20]. To formulate the system mathematically, we take the Cartesian coordinate system with the x and y axes in the plane of the rigid lower boundary and the z axis vertically upwards. Then the lower boundary is given by $z = 0$ and the upper free surface at the undisturbed state is located at $z = L$. When motion occurs the upper free surface of the liquid

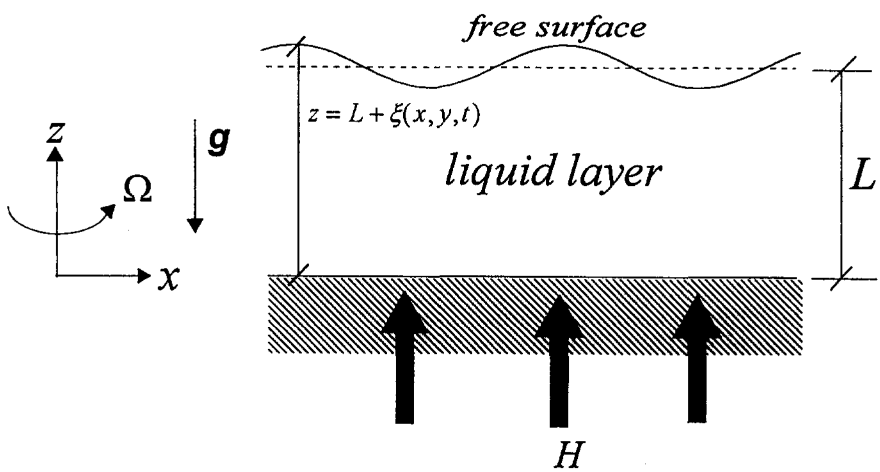

Fig. 1. Physical model.

layer will be deformably with its position at $z = L+\xi(x,y,t)$.

A set of dimension $[L, L^2/\kappa, \kappa/L, \Delta T, \kappa/L^2]$ is chosen for coordinates (x,y,z), time (t), velocity (w'), temperature (θ') and vertical vorticity (ζ'), respectively. The perturbation quantities in normal mode forms are

$$\begin{bmatrix} w' \\ \theta' \\ \zeta' \\ \xi \end{bmatrix} = \begin{bmatrix} W(z) \\ \Theta(z) \\ \zeta(z) \\ Z \end{bmatrix} \exp[i(a_x x + a_y y) + \sigma t] \quad (3)$$

where a_x and a_y are wavenumbers of disturbances in the x and y directions, respectively. W, Θ, ζ and Z are amplitudes of vertical velocity, temperature, vertical vorticity and deflection of the free upper surface, respectively. The governing equations of the perturbed state in dimensionless forms, assuming the Boussinesq approximation, are

$$\left[\frac{i\sigma_i}{Pr} - (D^2-a^2)\right]\zeta = \mathscr{T}^{1/2} DW \quad (4)$$

$$\left[\left(D^2-a^2-\frac{i\sigma_i}{Pr}\right)(D^2-a^2) - QD^2\right]W - \mathscr{T}^{1/2}D\zeta = a^2 R\Theta \quad (5)$$

$$[i\sigma_i - (D^2-a^2)]\Theta - W = 0 \quad (6)$$

where $D = \partial/\partial z$ and $a = \sqrt{a_x^2+a_y^2}$ is the wavenumber. The Prandtl number Pr, Rayleigh number R, Chandrasekhar number Q and Taylor number $\mathscr{T}$ are defined, respectively, as

$$Pr = \nu/\kappa, \quad R = \alpha g \Delta T L^3/\nu\kappa,$$

$$Q = \mu H^2 L^2/\rho\nu\eta, \quad \mathscr{T} = 4\Omega^2 L^4/\nu^2. \quad (7)$$

The boundary conditions at the deformably free upper surface, at $z = 1$, are

$$W = i\sigma_i Z \quad (8a)$$

$$(D+Bi)\Theta = Bi\, Z \quad (8b)$$

$$(D^2+a^2)W + Ma^2\Theta - Ma^2 Z = 0 \quad (8c)$$

$$C\left[\frac{i\sigma_i}{Pr} - (D^2-3a^2) + Q\right]DW + (Bo+a^2)a^2 Z + C\mathscr{T}^{1/2}\zeta = 0 \quad (8d)$$

$$D\zeta = 0 \quad (8e)$$

where the Crispation number C, Biot number Bi, Bond number Bo and Marangoni number M are defined, respectively, as

$$C = \rho\nu\kappa/\gamma L, \quad Bi = hL/K,$$

$$Bo = \rho g L^2/\gamma, \quad M = \tau \Delta T L/\rho\nu\kappa. \quad (9)$$

The lower boundary at $z = 0$ is rigid and isothermal,

$$W = DW = \Theta = \zeta = 0. \quad (10)$$

NUMERICAL PROCEDURE

The governing equations (4)–(6) and boundary conditions (8a)–(8e) and (10) form a Sturm–Liouville's problem with the Marangoni number M being the eigenvalue and other physical parameters R, Pr, $\mathscr{T}$, Q, C, Bo, Bi and a fixed. The modified shooting technique [23, 24], based on the fourth order Runge–Kutta–Gill's method, is used to solve the problem. Rewriting equations (4)–(6) to a system of first-order equations, we set, for the liquid layer,

$$W = u_1$$

$$DW = Du_1 = u_2 \quad (11a)$$

$$D^2W = Du_2 = u_3 \quad (11b)$$

$$D^3W = Du_3 = u_4 \quad (11c)$$

$$\Theta = u_5$$

$$D\Theta = Du_5 = u_6 \quad (11d)$$

$$\zeta = u_7$$

$$D\zeta = Du_7 = u_8 \quad (11e)$$

and we obtain

$$D^4W = Du_4 = \left(\frac{i\sigma_i}{Pr} + 2a^2 + Q\right)u_3 - \left(\frac{i\sigma_i}{Pr} + a^2\right)a^2 u_1 + a^2 R u_5 + \mathscr{T}^{1/2} u_8 \quad (11f)$$

$$D^2\Theta = Du_6 = (i\sigma_i + a^2)u_5 - u_1 \quad (11g)$$

$$D^2\zeta = Du_8 = \left(\frac{i\sigma_i}{Pr} + a^2\right)u_7 - \mathscr{T}^{1/2}u_2. \quad (11h)$$

The shooting procedure starts from the upper boundary at $z = 1$, and tries to match the boundary conditions at the lower boundary at $z = 0$. The upper boundary conditions, in equations (8a)–(8e) at $z = 1$ can be expressed as

$$u_1 = \left[-\frac{3i\sigma_i C}{Bo+a^2} + \frac{\sigma_i^2 C}{(Bo+a^2)a^2\,Pr} - \frac{i\sigma_i C Q}{(Bo+a^2)a^2}\right]u_2 + \frac{i\sigma_i C}{(Bo+a^2)a^2}u_4 - \frac{i\sigma_i C\mathscr{T}^{1/2}}{(Bo+a^2)a^2}u_7 \quad (12a)$$

$$u_3 = \left[\frac{3a^2 i\sigma_i C}{Bo+a^2} - \frac{\sigma_i^2 C}{(Bo+a^2)\,Pr} - \frac{3a^2 M C}{Bo+a^2} - \frac{i\sigma_i M C}{(Bo+a^2)\,Pr} + \frac{i\sigma_i C Q}{Bo+a^2} - \frac{MCQ}{(Bo+a^2)\,Pr}\right]u_2 + \left[-\frac{i\sigma_i C}{Bo+a^2} + \frac{MC}{Bo+a^2}\right]u_4 - Ma^2 u_5 + \left[-\frac{MC\mathscr{T}^{1/2}}{Bo+a^2} + \frac{i\sigma_i C\mathscr{T}^{1/2}}{Bo+a^2}\right]u_7 \quad (12b)$$

$$u_6 = \left[-\frac{i\sigma_i Bi\,C}{(Bo+a^2)a^2\,Pr} - \frac{3Bi\,C}{Bo+a^2} - \frac{Bi\,C\,Q}{Bo+a^2}\right]u_2 + \frac{Bi\,C}{(Bo+a^2)a^2}u_4 - Bi\,u_5 - \frac{Bi\,C\,\mathscr{T}^{1/2}}{(Bo+a^2)a^2}u_7 \quad (12c)$$

$$u_8 = 0. \quad (12d)$$

We shall guess four boundary conditions,

$$u_2 = c_1, \quad u_4 = c_2, \quad u_5 = c_3, \quad \text{and} \quad u_7 = c_4. \quad (13)$$

Then the general form of the solution becomes

$$U = c_1 U_1 + c_2 U_2 + c_3 U_3 + c_4 U_4 \quad (14)$$

where

$$U = [u_1, u_2, u_3, u_4, u_5, u_6, u_7, u_8]^T \quad (15a)$$

$$U_1 = \left[-\frac{3i\sigma_i C}{Bo+a^2} + \frac{\sigma_i^2 C}{(Bo+a^2)a^2\,Pr} - \frac{i\sigma_i C Q}{(Bo+a^2)a^2}, 1, \frac{3a^2 i\sigma_i C}{Bo+a^2} - \frac{i\sigma_i C}{(Bo+a^2)\,Pr} - \frac{3a^2 M C}{Bo+a^2} - \frac{i\sigma_i M C}{(Bo+a^2)\,Pr} + \frac{i\sigma_i C Q}{Bo+a^2} - \frac{M C Q}{(Bo+a^2)\,Pr}, 0, 0, -\frac{i\sigma_i Bi\,C}{(Bo+a^2)a^2\,Pr} - \frac{3Bi\,C}{Bo+a^2} - \frac{Bi\,C\,Q}{(Bo+a^2)a^2}, 0, 0\right]^T \quad (15b)$$

$$U_2 = \left[\frac{i\sigma_i C}{Bo\,a^2 + a^4}, 0, -\frac{i\sigma_i C}{Bo+a^2} + \frac{M C}{Bo+a^2}, 1, 0, -\frac{Bi\,C}{(Bo+a^2)a^2}, 0, 0\right]^T \quad (15c)$$

$$U_3 = [0, 0, -M a^2, 0, 1, -Bi, 0, 0]^T \quad (15d)$$

$$U_4 = \left[-\frac{i\sigma_i C\,\mathscr{T}^{1/2}}{(Bo+a^2)a^2}, 0, -\frac{M\,i\sigma_i C\,\mathscr{T}^{1/2}}{(Bo+a^2)} + \frac{i\sigma_i C\,\mathscr{T}^{1/2}}{(Bo+a^2)}, 0, 0, \frac{Bi\,C\,\mathscr{T}^{1/2}}{(Bo+a^2)a^2}, 1, 0\right]^T. \quad (15e)$$

We may guess a value for M and assume each of $U_{i,i=1,2,3,4}$ in equations (15b)–(15e) as a set of initial conditions. We then start the shooting procedure, using the Runge–Kutta–Gill's method of order four, from $z = 1$ and try to match the lower boundary conditions at $z = 0$. The results finally turn into a matrix form,

$$\begin{bmatrix} U_1^1 & U_2^1 & U_3^1 & U_4^1 \\ U_1^2 & U_2^2 & U_3^2 & U_4^2 \\ U_1^5 & U_2^5 & U_3^5 & U_4^5 \\ U_1^7 & U_2^7 & U_3^7 & U_4^7 \end{bmatrix} \begin{bmatrix} c_1 \\ c_2 \\ c_3 \\ c_4 \end{bmatrix} = 0 \quad (16)$$

where the superscript indicates the element of $U_{i,i=1,2,3,4}$. The determinant in equation (16) is complex, but its real and imaginary parts should vanish for c_i being nontrivial. The eigenvalue problem is established as

$$f(i\sigma_i, R, M, Pr, \mathscr{T}, Q, C, Bo, Bi, a) = 0 \quad (17)$$

where f is the determinant of the coefficient matrix.

The equation (17) can be solved directly, using the iterative Broyden's method [23, 24], and the eigenvalue and the frequency σ_i are thus obtained. An initial approximation $\mathbf{x}^{(0)} = (x_1, x_2)^T = [M, i\sigma_i]^T$ (or $[R, i\sigma_i]^T$) and the Jacobian matrix $J(\mathbf{x}^{(0)})$ are needed, where

$$J(\mathbf{x}^{(0)}) = J(\mathbf{x})_{i,j} = \frac{\partial f_i(\mathbf{x})}{\partial x_j}, \quad \text{for} \quad i,j = 1,2. \quad (18)$$

Then a corrected matrix $A^{(0)} = J(\mathbf{x}^{(0)})$ gives rise to the result,

$$\mathbf{x}^{(1)} = \mathbf{x}^{(0)} - [A^{(0)}]^{-1} f(\mathbf{x}^{(0)}). \quad (19)$$

In each step following (n), we obtain a newly corrected matrix,

$$[A^{(n)}]^{-1} = [A^{(n-1)}]^{-1} + \frac{\{\mathbf{s}^{(n)} - [A^{(n-1)}]^{-1}\mathbf{y}^{(n)}\}[\mathbf{s}^{(n)}]^T[A^{(n-1)}]^{-1}}{[\mathbf{s}^{(n)}]^T[A^{(n-1)}]^{-1}\mathbf{y}^n} \quad (20)$$

where $\mathbf{y}^{(n)} = f(\mathbf{x}^{(n)}) - f(\mathbf{x}^{(n-1)})$ and $\mathbf{s}^{(n)} = \mathbf{x}^{n)} - \mathbf{x}^{(n-1)}$. The new approximation is then achieved iteratively.

$$\mathbf{x}^{(n+1)} = \mathbf{x}^{(n)} - [A^{(n)}]^{-1} f(\mathbf{x}^{(n)}). \quad (21)$$

The iteration is terminated when the determinant f is less than a tolerance. The critical Marangoni number M_c, being the minimum one on the marginal surfaces of the $(a, M, i\sigma)$ space, marks the onset of convective instability at the marginal state. The convection is stationary or oscillatory, depending on whether the σ_i is vanishing or nonvanishing.

RESULTS AND DISCUSSION

In order to validate the above numerical algorithm, we first concentrate on the Marangoni instability problem without the thermal buoyancy (i.e., $R = 0$). For the Crispation number C in the range 10^{-6}–10^{-1}, the present results of M_c, a_c and σ_{ic} are calculated and very well compared with those previous ones [12], as listed in Table 1 for the case of $Pr = 1$, $Bo = 0.1$ and $Bi = 0$. A negative value of Marangoni number, $M < 0$, related to an increasing surface tension with an increasing temperature, has been shown and predicted to be a main factor of causing the appearance of oscillatory modes for the pure Marangoni convection

Table 1. Numerically calculated values of M_c, a_c and σ_{ic} for different values of C and Pr on the oscillatory instability of Marangoni convection without the thermal buoyancy and the magnetic field. ($Bo = 0.1$, $Bi = 0$ and $\mathscr{T} = Q = R = 0$)

	Data of [12] $Pr = 1.0$			Present study $Pr = 1.0$			Present study $Pr = 0.1$		
C	M_c	a_c	σ_{ic}	M_c	a_c	σ_{ic}	M_c	a_c	σ_{ic}
0	—	—	—	—	—	—	—	—	—
10^{-6}	−62785.97	0.08	26	−62785.117	0.080	26.106	−27339.290	0.073	7.551
10^{-5}	−8554.13	0.18	21	−8552.231	0.178	20.775	− 3331.287	0.131	4.561
10^{-4}	−1896.11	0.34	17	−1895.632	0.346	16.551	−545.415	0.232	3.010
10^{-3}	−1075.92	0.59	17	−1075.895	0.591	16.610	−144.761	0.391	2.216
10^{-2}	−1044.56	0.28	6.7	−1043.880	0.283	6.753	−70.086	0.517	1.572
10^{-1}	−1016.23	0.28	6.7	−1015.898	0.282	6.584	−65.541	0.538	1.316

[12, 16, 21]. For the reason, no oscillatory modes were found for $M > 0$. The critical Marangoni number in the absolute form $|M_c|$ and its associated frequency σ_{ic} as functions of the Crispation number C for selected values of the Prandtl number Pr are plotted in Fig. 2(a) and 2(b). here we choose $Bo = 0.1$ and $Bi = R = Q = \mathscr{T} = 0$. The results show that the critical conditions $|M_c|$ and σ_{ic} do decrease with the Crispation number C. The Crispation number C, associated with the inverse effect of the surface tension, shows the rigidity of the free upper surface. For the Crispation number C vanishing, the upper surface, subject to an infinite surface tension, is free and flat, the system becomes more stabilizing such that the pure Marangoni instability sets in stationarily. For oscillatory modes to be possible, larger values of the Crispation number C, allowing the free upper surface to deform, are required to achieve smaller values of $|M_c|$. As well, influences of the Prandtl number Pr on the existence of oscillatory convection of the pure Marangoni instability are important, since the increasing viscosity would suppress the possible convection of Rayleigh–Bénard instability, even irrespective of the Crispation number C. The critical conditions $|M_c|$ and σ_{ic}, as shown in Fig. 2(a) and (b), increase with the Prandtl number Pr.

In Table 2, a set of physically realistic values, $C = 10^{-5}$, $Pr = 0.02$ and $Bo = 10^{-2}$, is chosen and the results are compared with those previous ones [21], here the range of the Chandrasekhar number Q is 0–50. Figure 3(a) and (b) shows the critical conditions $|M_c|$ and σ_{ic} as functions of the Chandrasekhar number Q for selected values of the Biot number Bi, here we choose $C = 10^{-5}$, $Pr = 0.02$, $Bo = 10^{-2}$ and $R = \mathscr{T} = 0$. The critical conditions $|M_c|$ and σ_{ic} increase monotonically with the Chandrasekhar number Q, as predicted [17–22], since the presence of the magnetic field acts as a stabilizing effect. Thermally, the more the thermal energy is conducted away, the less it is stored in the fluid layer so that the system become more stabilizing. Also a perfectly insulated upper surface, $Bi = 0$, would totally prevent the thermal dissipation into the ambient surrounding, in contrast to an isothermal one, $Bi \to \infty$. Therefore, a larger value of the Biot number Bi would lead to a higher value of $|M_c|$ and, as well, a larger value of σ_{ic}.

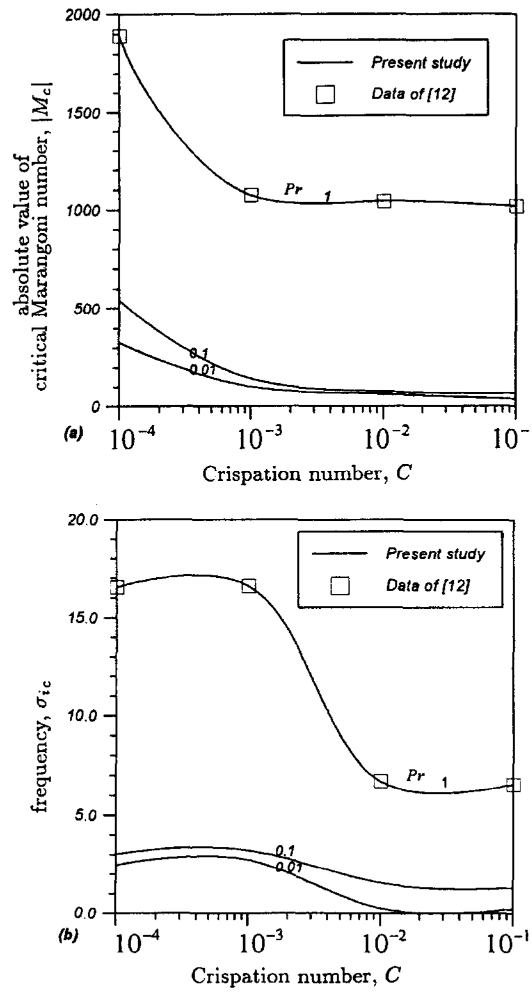

Fig. 2. Variations of critical conditions (a) $|M_c|$ and (b) σ_{ic} are plotted as function of C for several values of Pr on the oscillatory Marangoni instability for $Bo = 0.1$ and $Bi = R = Q = \mathscr{T} = 0$.

Figure 4(a) and (b) shows the critical conditions

Table 2. Numerically calculated values of M_c, a_c and σ_{ic} for different values of Q and Bi on the oscillatory instability of Marangoni convection without the thermal buoyancy. ($C = 10^{-5}$, $Pr = 0.02$, $Bo = 10^{-2}$, and $\mathcal{T} = R = 0$)

	$Bi = 0$			$Bi = 0.05$			$Bi = 0.1$		
Q	M_c	a_c	σ_{ic}	M_c	a_c	σ_{ic}	M_c	a_c	σ_{ic}
0	−952.403	0.2015	2.0863	−1027.587	0.2071	2.1914	−1105.408	0.2126	2.2972
	(−952.41	0.2015	2.0864)	(−1027.60	0.2071	2.1916)			
1	−1094.296	0.2114	2.2808	−1177.988	0.2170	2.3909	−1264.527	0.2225	2.5018
	(−1094.31	0.2114	2.2803)	(−1177.01	0.2170	2.3912)			
5	−1666.793	0.2380	2.8633	−1784.995	0.2442	3.0002	−1906.802	0.2504	3.1402
9	−2267.356	0.2574	3.3418	−2421.210	0.2643	3.5063	−2579.370	0.2712	3.6746
	(−2267.37	0.2574	3.3414)	(−2421.23	0.2643	3.5065)			
10	−2423.121	0.2618	3.4562	−2586.102	0.2689	3.6282	−2753.556	0.2759	3.8019
20	−4120.799	0.3019	4.5906	−4379.575	0.3107	4.8350	−4644.101	0.3195	5.0855
25	−5070.047	0.3214	5.1951	−5378.867	0.3310	5.4780	−5693.599	0.3407	5.7707
	(−5070.04	0.3214	5.1941)	(−5378.86	0.3310	5.4783)			
49	−10464.891	0.4224	8.7969	−10989.154	0.4364	9.3186	−11512.085	0.4506	9.8610
	(−10464.89	0.4224	8.7974)	(−10989.154	0.4364	9.3204)			
50	−10712.039	0.4270	8.9778	−11243.077	0.4412	9.5116	−11772.261	0.4555	10.0629

The values in ( ) are obtained from Wilson [21].

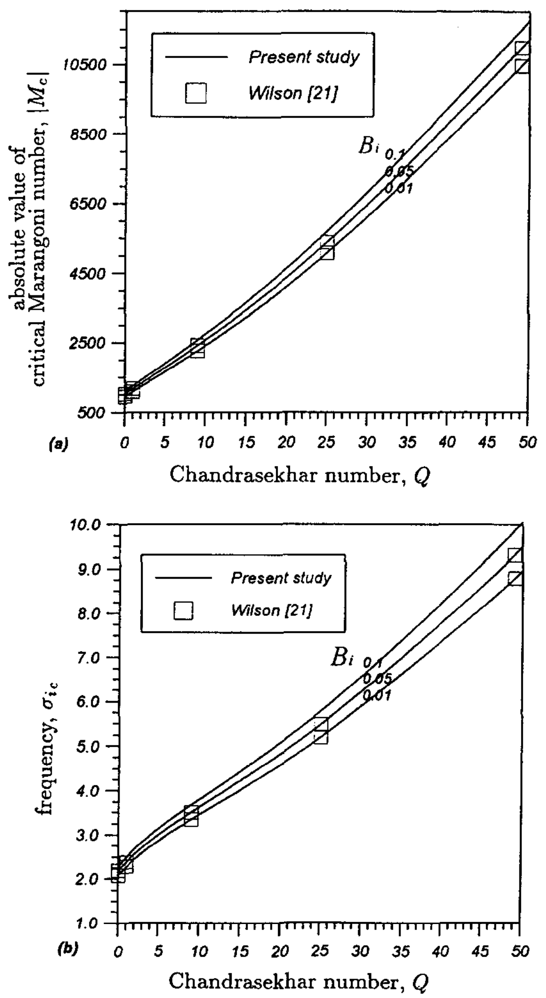

Fig. 3. Variations of critical conditions (a) $|M_c|$ and (b) σ_{ic} are plotted as function of Q for several values of Bi on the oscillatory Marangoni instability for $C = 10^{-5}$, $Pr = 0.02$, $Bo = 10^{-2}$ and $R = \mathcal{T} = 0$.

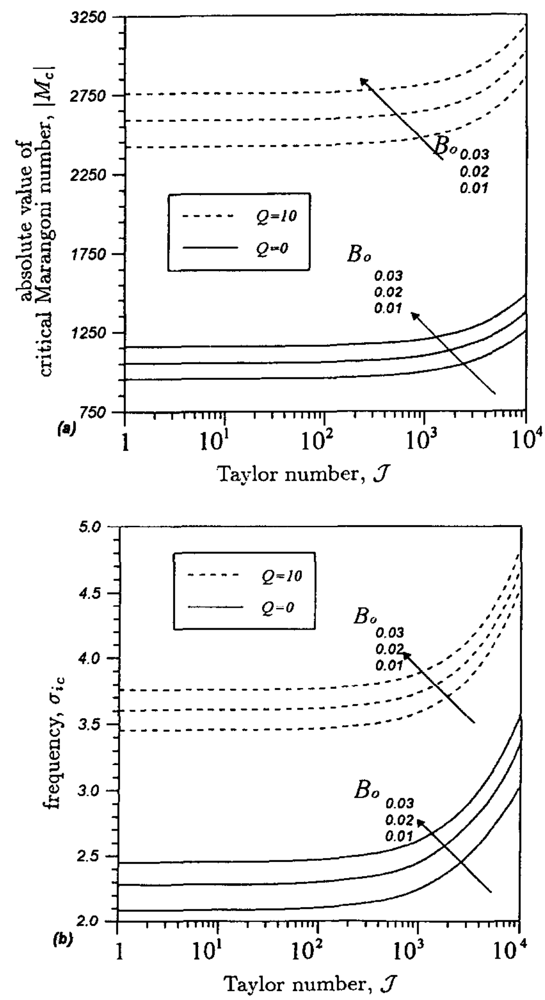

Fig. 4. Variations of critical conditions (a) $|M_c|$ and (b) σ_{ic} are plotted as function of $\mathcal{T}$ for several values of Bo on the oscillatory Marangoni instability for $C = 10^{-5}$, $Pr = 0.02$, $Bi = R = 0$.

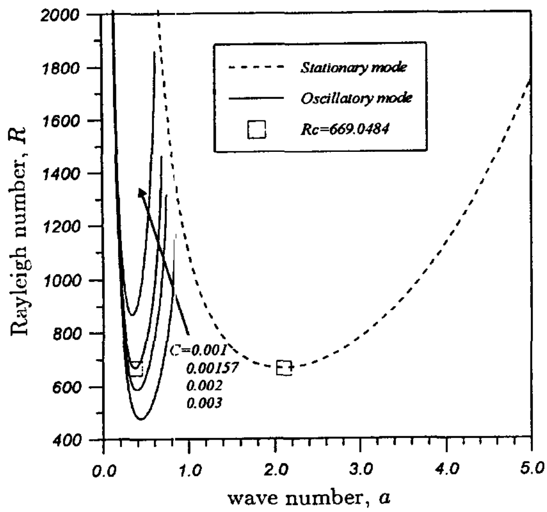

Fig. 5. The marginal curves $R(a)$ are plotted for several values of C on the stability of the Rayleigh–Bénard convection for $Pr = 1$, $Bo = 0.1$, and $Bi = M = Q = \mathscr{T} = 0$.

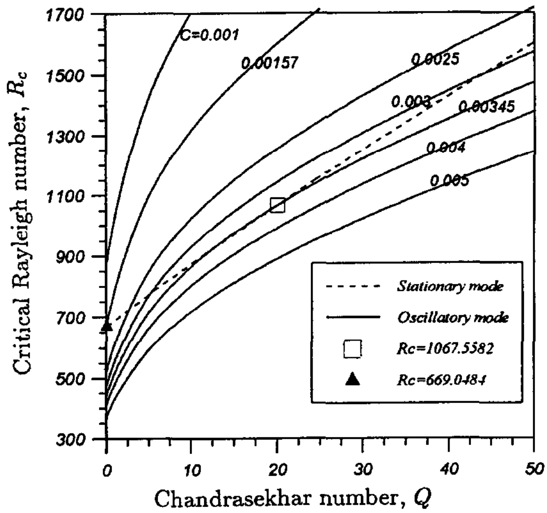

Fig. 6. Variations of critical conditions R_c are plotted as function of Q for several values of C on the stability of the Rayleigh–Bénard convection for $Pr = 1$, $Bo = 0.1$, and $Bi = M = \mathscr{T} = 0$.

$|M_c|$ and σ_{ic} plotted as functions of $\mathscr{T}$ for selected values of the Bond number Bo and the Chandrasekhar number Q, here we choose $C = 10^{-5}$, $Pr = 0.02$ and $Bi = R = 0$. The critical conditions $|M_c|$ and σ_{ic} increase with the Taylor number $\mathscr{T}$, as predicted by the Taylor–Proudman theorem [1] that all steady slow motions of inviscid flow in a rotating system are necessarily two dimensional. The effect of rotation suppresses the onset of the convection and raises the stability of the system. The Bond number Bo illustrates the relative effect of gravity to surface tension on flattening a deformably free surface. For a fixed Crispation number C, the effect of gravity force is intensified, as the Bond number Bo increases. As shown in Fig. 4(a), the critical condition $|M_c|$ increases sensitively with the Bond number Bo.

For the pure Rayleigh–Bénard instability, $M = 0$, the corresponding marginal curves of stationary and oscillatory modes versus the wavenumber a are plotted in Fig. 5 for selected values of the Crispation number C, here we choose $Pr = 1$, $Bo = 0.1$ and $Bi = M = Q = \mathscr{T} = 0$. The stationary modes is shown to be insensitive to the Crispation number C, in contrast to the oscillatory modes. The critical Rayleigh number R_c of oscillatory modes decreases as the Crispation number C increases. For the stationary mode, the critical conditions R_c and a_c are 669.0484 and 2.086, respectively, which coincides exactly with the previous results [1, 3]. There always exists a Crispation number C_{so} such that, for $C > C_{so}$, the minimum Rayleigh number R for the oscillatory mode is smaller than that for the stationary mode and the pure Rayleigh–Bénard instability sets in oscillatory, where $C_{so} = 1.57 \times 10^{-3}$ for $Pr = 1$, $Bo = 0.1$ and $Bi = Q = \mathscr{T} = 0$.

Figure 6 shows the critical Rayleigh number R_c of stationary and oscillatory modes as a function of the Chandrasekhar number Q for selected values of C, here we choose $Pr = 1$, $Bo = 0.1$ and $Bi = M = \mathscr{T} = 0$. As the Crispation number C increases, the reducing surface tension acts as a destabilizing effect to oscillatory modes. Also shown in Fig. 6, under the stabilizing effect of the magnetic field, there exist jumps on the Rayleigh–Bénard instability from stationary modes to oscillatory modes, depending on the Chandrasekhar number Q, for $Q = 0$, $C_{so} = 1.57 \times 10^{-3}$, and for $Q = 20$, $C_{so} = 3.45 \times 10^{-3}$.

The critical conditions $|M_c|$ and frequency σ_{ic} vs the Rayleigh number R for various values of $\mathscr{T}$ are plotted in Fig. 7(a) and (b), and listed in Table 3 with $Q = 0, 10$, here we choose $C = 10^{-5}$, $Pr = 0.02$, $Bo = 10^{-2}$, $Bi = 0$ and $R = 0$–1000. Taking into account effects of thermal buoyancy and surface tension, marginal curves on the $(|M_c|, R)$-plane do satisfy, for both stationary and oscillatory modes, the linear relation of the decreasing $|M_c|$ with the increasing Rayleigh number R, irrespective of the Taylor number $\mathscr{T}$. As shown in Fig. 7(b), the critical frequency σ_{ic} decreases monotonically with the Rayleigh number R, provided $Q = 10$, at which the magnetic field is the dominant stabilizing effect, however, it becomes very insensitive, provided $Q = 0$.

CONCLUSIONS

The onset of stationary and oscillatory modes of Bénard–Marangoni instability subject to effects of rotation and magnetic field is analyzed numerically. The following results have been obtained.

1. For the pure Marangoni convection, oscillatory modes could take place for negative values of the Marangoni number M only. For the Crispation number $C > 1.57 \times 10^{-3}$, there exist jumps on the

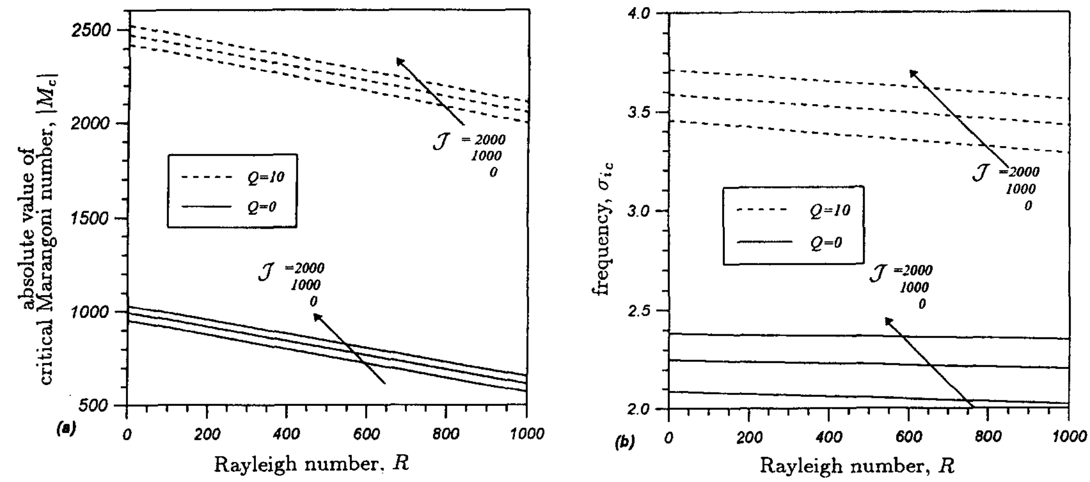

Fig. 7. Variations of critical conditions (a) $|M_c|$ and (b) σ_{ic} are plotted as function of R for several values of $\mathcal{T}$ on the oscillatory Bénard–Marangoni instability for $C = 10^{-5}$, $Pr = 0.02$, $Bo = 10^{-2}$ and $Bi = 0$.

Table 3. Critical values of Marangoni number M_c, a_c and σ_{ic} for different values of R and $\mathcal{T}$ on the oscillatory instability of the Bénard–Maragoni convection ($C = 10^{-5}$, $Pr = 0.02$, $Bo = 10^{-2}$ and $Bi = 0$)

	$Q = 0$								
	$\mathcal{T} = 0$			$\mathcal{T} = 1000$			$\mathcal{T} = 2000$		
R	M_c	a_c	σ_{ic}	M_c	a_c	σ_{ic}	M_c	a_c	σ_{ic}
0	−952.403	0.2015	2.0863	−994.175	0.2057	2.2490	−1031.131	0.2086	2.3826
100	−914.442	0.2016	2.0809	−956.511	0.2059	2.2455	−993.712	0.2088	2.3793
200	−876.464	0.2016	2.0737	−918.837	0.2060	2.2403	−956.286	0.2090	2.3759
300	−838.471	0.2017	2.0682	−881.153	0.2062	2.2368	−918.852	0.2092	2.3725
400	−800.463	0.2017	2.0610	−843.458	0.2063	2.2315	−881.410	0.2095	2.3708
500	−762.438	0.2018	2.0554	−805.752	0.2065	2.2279	−843.960	0.2097	2.3673
600	−724.397	0.2018	2.0482	−768.036	0.2066	2.2226	−806.503	0.2099	2.3639
700	−686.341	0.2019	2.0426	−730.310	0.2068	2.2189	−769.038	0.2102	2.3621
800	−648.268	0.2019	2.0352	−692.573	0.2069	2.2135	−731.566	0.2104	2.3586
900	−610.178	0.2020	2.0295	−654.826	0.2071	2.2098	−694.086	0.2106	2.3550
1000	−572.072	0.2020	2.0221	−617.069	0.2072	2.2044	−656.599	0.2108	2.3515

	$Q = 0$								
	$\mathcal{T} = 0$			$\mathcal{T} = 1000$			$\mathcal{T} = 2000$		
R	M_c	a_c	σ_{ic}	M_c	a_c	σ_{ic}	M_c	a_c	σ_{ic}
0	−2423.121	0.2618	3.4562	−2474.677	0.2653	3.5902	−2523.837	0.2685	3.7154
100	−2381.048	0.2614	3.4397	−2433.026	0.2649	3.5738	−2482.562	0.2681	3.6991
200	−2338.937	0.2610	3.4231	−2391.342	0.2645	3.5574	−2441.258	0.2678	3.6850
300	−2296.786	0.2605	3.4044	−2349.625	0.2641	3.5409	−2399.926	0.2674	3.6687
400	−2254.595	0.2601	3.3878	−2307.873	0.2638	3.5267	−2358.564	0.2671	3.6546
500	−2212.364	0.2597	3.3712	−2266.087	0.2634	3.5102	−2317.173	0.2667	3.6383
600	−2170.091	0.2593	3.3546	−2224.266	0.2630	3.4938	−2275.752	0.2664	3.6241
700	−2127.776	0.2589	3.3380	−2182.409	0.2626	3.4774	−2234.301	0.2660	3.6078
800	−2085.419	0.2585	3.3214	−2140.516	0.2622	3.4609	−2192.819	0.2657	3.5937
900	−2043.018	0.2580	3.3027	−2098.587	0.2618	3.4445	−2151.306	0.2653	3.5774
1000	−2000.574	0.2576	3.2861	−2056.621	0.2614	3.4281	−2109.761	0.2649	3.5611

Rayleigh–Bénard instability from stationary modes to oscillatory modes, depending on the Chandrasekhar number Q.

2. The deformation of the upper surface does have significant influences on the occurrence of oscillatory modes of the Bénard–Marangoni instability. Smaller critical conditions $|M_c|$ and σ_{ic} take place at larger values of the Crispation number C.

3. Effects of rotation and magnetic field do suppress the onset of convection and act as the stabilizing factors to the system.
4. The system becomes more stabilizing, when the Biot number Bi and the Bond number Bo increase. The influences of the Prandtl number Pr on the existence of oscillatory convection of the pure Marangoni instability are important. The critical conditions $|M_c|$ and σ_{ic} increase with the Prandtl number Pr.
5. Marginal curves on the $(|M_c|, R)$-plane do satisfy the linear relation of the decreasing $|M_c|$ with the increasing Rayleigh number R, irrespective of the Taylor number.

Acknowledgement—The author gratefully acknowledges the support of the National Science Council, Republic of China, through the project NSC 87-2212-E-164-001.

REFERENCES

1. Chandrasekhar, S., *Hydrodynamic and Hydromagnetic Stability*. Oxford University Press, London, 1961.
2. Drazin, P. G. and Reid, W. H., *Hydrodynamic Stability*. Oxford University Press, London, 1961.
3. Sparrow, E. M., Goldstein, R. J. and Jonsson, V. K., Thermal instability in a horizontal fluid layer: effect of boundary conditions and non-linear temperature, 1964, **18,** 513–528.
4. Ferm, E. N. and Wollkind, D. J., Onest of Rayleigh–Bénard–Marangoni instability: comparison between theory and experiments. *Journal of Non-Equilibrated Thermodynamics*, 1982, **9,** 169–170.
5. Pearson, J. R. A., On convection cell induced by surface tension. *Journal of Fluid Mechanics*, 1958, **4,** 489–500.
6. Vidal, A. and Acrivos, A., Nature of the neutral state in surface-tension driven convection. *Physics of Fluids*, 1966, **9,** 615–616.
7. Nield, D. A., Surface tension and buoyancy effects in cellular convection. *Journal of Fluid Mechanics*, 1964, **19,** 341–352.
8. Scriven, L. E. and Sternling, C. V., On cellular convection driven by surface tension gradients: effect of mean surface tension and surface viscosity. *Journal of Fluid Mechanics*, 1965, **19,** 321–340.
9. Smith, K. A., On convective instability induced by surface-tension gradients. *Journal of Fluid Mechanics*, 1966, **24,** 401–414.
10. Davis, S. H. and Homsy, G. M., Energy stability theory for free-surface problem: buoyancy-thermocapillary layers. *Journal of Fluid Mechanics*, 1980, **98,** 527–553.
11. Benguria, R. D. and Depassier, M. C., On the linear stability theory of Bénard–Marangoni convection. *Physics of Fluids*, 1989, **1**(6), 1123–1127.
12. Pérez-García, C. and Carneiro, G., Linear stability analysis of Bénard–Marangoni convection in fluids with a deformable free surface. *Physics of Fluids*, 1991, A **3**(2), 292–298.
13. Veronis, G., Motions at subcritical values of the Rayleigh number in a rotating fluid. *Journal of Fluid Mechanics*, 1966, **24,** 545–554.
14. Friedrich, R. and Rudraiah, N., Marangoni convection in a rotating fluid layer with non-uniform temperature gradient. *International Journal of Heat and Mass Transfer*, 1984, **27,** 443–449.
15. Pearlstein, A. J., Effect of rotation on the stability of a doubly diffusive fluid layer. *Journal of Fluid Mechanics*, 1981, **103,** 389–412.
16. Sarma, G. R. S., On oscillatory modes of thermocapillary instability in a liquid layer rotating about a transverse axis. *Physico-Chemical Hydrodynamics*, 1981, **2,** 143–151.
17. Sarma, G. R. S., Effects of interfacial curvature and gravity waves on the onset of thermocapillary convective instability in a rotating liquid layer subjected to a transverse magnetic field. *Physico-Chemical Hydrodynamics*, 1985, **6,** 283–300.
18. Maekawa, T. and Tanasawa, I., Effect of magnetic field on onset of Marangoni convection. *International Journal of Heat and Mass Transfer*, 1988, **31,** 285–293.
19. Maekawa, T. and Tanasawa, I., Effect of magnetic field and buoyancy on onset of Marangoni convection. *International Journal of Heat and Mass Transfer*, 1989, **32,** 1377–1380.
20. Wilson, S. K., The effect of a uniform magnetic field on the onset of steady Bénard-Marangoni convection in a layer of conducting fluid. *Journal of Engineering Mathematics*, 1993, **27,** 161–188.
21. Wilson, S. K., The effect of a uniform magnetic field on oscillatory Marangoni convection. *Microgravity Scientific Technology*, 1994, **VII/3,** 228–233.
22. Wilson, S. K., The effect of a uniform magnetic field on the onset of steady Maragoni convection in a layer of conducting fluid with a prescribed heat flux at its lower boundary. *Physics of Fluids*, 1994, **6**(11), 3591–3600.
23. Davey, A., Numerical methods for the solution of linear differential eigenvalue problem. University of Newcastle-upon-Tyne Press, Newcastle-upon-Tyne, 1976, 485–498.
24. Burden, R. L. and Fairs, J. D., *Numerical Analysis*. Prindle, Weber and Schmidt Publishers, Boston, 1985.